Energy Harvesting Pixel Array with Deep Trench Isolated Diodes for Self-Powered Imaging

F. Kaklin[1,2], J. M. Raynor[2], R. K. Henderson[1]
[1]School of Engineering, Institute for Integrated Micro and Nano Systems, The University of Edinburgh, Filip.Kaklin@ed.ac.uk
[2]STMicroelectronics Imaging Division, Edinburgh, UK

Abstract—An array of pixels with dual functionality is implemented in a deep trench isolation (DTI), backside illuminated (BSI) process. Full thickness isolation separates the diode from the readout and reconfiguration transistors to make a 4T pixel. Each row of the array can operate independently in imaging mode (IM) or energy harvesting (EH) mode, ensuring power generation even when capturing a frame. The theoretical limit for power generation is evaluated based on an idealized lens and realistic illumination levels for different spectra. The presented chip achieves around half of this limit, operating with an efficiency between 9-15%.

I. Introduction

The two operating regions of illuminated diodes, namely photoconductive mode and photovoltaic mode, make them uniquely capable of sensing and power generation. Using both modes within the same physical device is tempting as it promises a net zero power sensor in a very small form factor.

In [1], the proposed energy harvesting and imaging (EHI) pixel uses a p+/nwell/p-sub diode where the two pn junctions work in parallel while imaging, and the nwell is grounded during energy harvesting to develop a positive voltage at the p+ diffusion. The shallow diffusion junction, however, is not an efficient energy harvesting structure. Alternative pixels presented in [2], [3] use the deeper and lower doped nwell/p-sub junction for EH and achieve an order of magnitude improvement in generated power, but the voltage generated is negative with respect to the grounded substrate and a polarity inverting charge pump is needed to generate a positive supply rail. Voltage boosting circuits are present in many previous works [1]–[6] because the output voltage of the diode in EH mode is variable and at most ~0.5V. While some imagers are adapted to operate with low power supplies of 0.5V [7], and even down to 0.32V [8], the output of a single PV can fall below this level and many circuits would benefit from a higher voltage bias being available.

Previous implementations of EHI pixels apply the same operating mode to the entire array, not imaging when generating power, and cutting all power generation when imaging [1], [8]. Others attempted to maintain continuous power generation by fitting two diodes in each pixel [3], or use junctions at different depths [4] to utilise part of the light for imaging, and the remainder for power generation. For the imager presented in this work, DTI enables a new, row level control over the operating mode of the pixels that ensures power generation is never entirely interrupted.

This paper also looks at the theoretical limits of energy harvesting using an image sensor and the benefits of using BSI and DTI.

II. Theoretical Limit

The starting point to finding the theoretical limit for power generation is establishing the range of focal plane illumination, E_i. Knowing the illumination on a target scene E_s and its reflectance R we can use:

$$E_i = \frac{E_s R}{\pi} T_x \frac{\pi}{4} \left(\frac{1}{F}\right)^2,$$

where T_x is the transmittance of the lens and any filters, and F is the lens focal length to aperture diameter ratio. The $E_s R/\pi$ factor is the scene luminance, alternatively denoted with L. The photometric illumination E can be replaced with its radiometric equivalent, irradiance.

At the high end of the range consider the optimistic case of a 50% reflective target illuminated with direct sunlight at 100klux, and imaged using an f/1.5 lens with 95% transmission. The illuminance at the focal plane will then be 5.3klux.

From this, the peak available power per unit area can be calculated using the equation

$$P = E_e \eta(E_e, \lambda).$$

It is important to recognize that η, the photovoltaic conversion efficiency, increases logarithmically with irradiance E_e, and depends on the incident wavelength denoted by λ.

In this paper, the energy harvesting performance is tested at light levels realistic for operation with a lens, and using three different spectra of light: a close fit to the standard AM1.5 solar spectrum, a D65 illuminant, and a 5700K LED. Figure 1 shows the spectra normalized to 1000 lux, and their relative power distribution in four different wavelength bands is listed in Table 1.

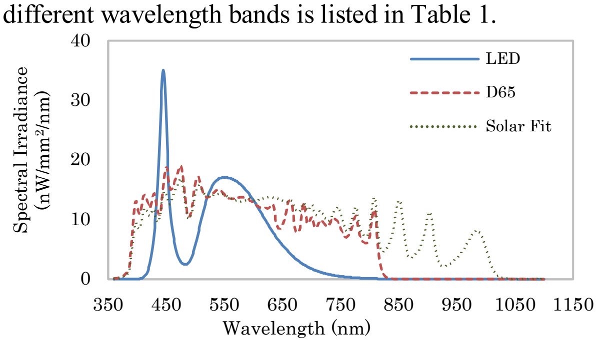

Figure 1: Broadband spectra used for power generation characterization.

Spectrum	UV	Visible	NIR	>E_g	Irradiance	η_{peak}
λ (nm)	<380	380-780	780-1127	>1127	($\mu W/mm^2$)	(%)
LED	-	100	-	-	3.02	26.4
D65	-	94	6	-	5.09	28.7
Solar Fit	<1	76	24	-	6.39	32.7
AM1.5	2.2	52	25	21	7.19	27.6

Table 1: Spectral power distribution in percent (%) of the three illuminants used, and reference Air Mass 1.5 spectrum, each at 1000 lux. The theoretical maximum photovoltaic conversion efficiency η_{peak} is also calculated for the given irradiance, for a 1.1eV bandgap material at 300K.

III. Test Chips

The test chip presented here was designed to verify the energy harvesting capabilities in this process technology alongside basic imaging operation as a precursor to a complete self-powered imager. We designed a new implementation of an energy harvesting and imaging pixel, with the diode separated from the readout transistors using a full thickness trench as shown in Figure 2. The readout is based on a 3T pixel, with an additional NMOS switch used to enable energy harvesting mode.

Four arrays with different diode doping profiles were reported in [9] and are directly comparable in terms of power generation thanks to their identical layout.

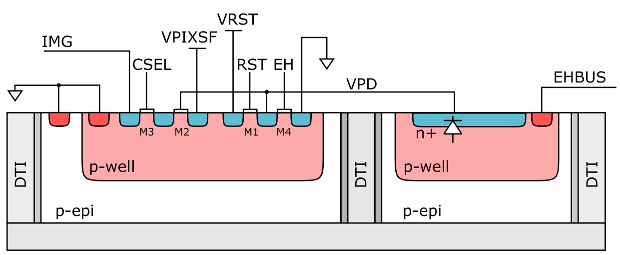

Figure 2: Cross-section of pixel, with control and readout transistors separated from the diode.

A. Benefits of full thickness DTI and BSI in EHI pixels

Full thickness trench isolation combines two mutually exclusive qualities of diodes from standard processes: the positive voltage generation of diffusion/well junctions, and the high power generation of nwell/psub junctions.

The pixel in Figure 2 can be switched into energy harvesting mode by connecting the n+ diffusion to ground through transistor M4. This causes the substrate to develop a positive voltage of approximately 0.45V under sufficient illumination, which can be used to provide power. Transistors placed in neighbouring, isolated substrate regions continue to operate with their local substrate grounded and are not affected thanks to the isolation.

Additionally, the diodes of multiple pixels can be arbitrarily chained together to generate a higher voltage, without using a boost circuit [9].

The isolation allows each pixel to be independently configured in either IM or EH mode. This property is used here to implement a new method of time-multiplexing the two operating modes that avoids interrupting energy harvesting operation.

Backside illumination benefits energy harvesting pixels in similar ways that it does imaging pixels. Firstly it increases the light collection area through better fill factor, directly increasing power generation. Secondly it increases the quantum efficiency for longer wavelengths, which translates to an overall improved photovoltaic conversion efficiency.

B. Array Operation

A single EH-DTI pixel was laid out to a 22.4µm pitch, using a 7×7 grid of 3.2µm pitch sub-pixels. One of the 49 discrete substrate regions is dedicated to holding the readout transistors, with the remaining 48 working as a single diode. A 32×32 test array of these pixels has been laid out, with row and column decoders for pixel-level addressing. Pixel outputs are sequentially multiplexed to a PMOS source follower output and an external ADC is used to digitize the signal.

A diagram of the chip is shown in Figure 3. All control and timing signals are generated off-chip.

During frame readout, a single row is enabled into imaging mode, while the remaining 31 rows continue to operate in energy harvesting mode. Diodes in all energy harvesting pixels are connected in parallel, and the output is brought off chip to a sourcemeter.

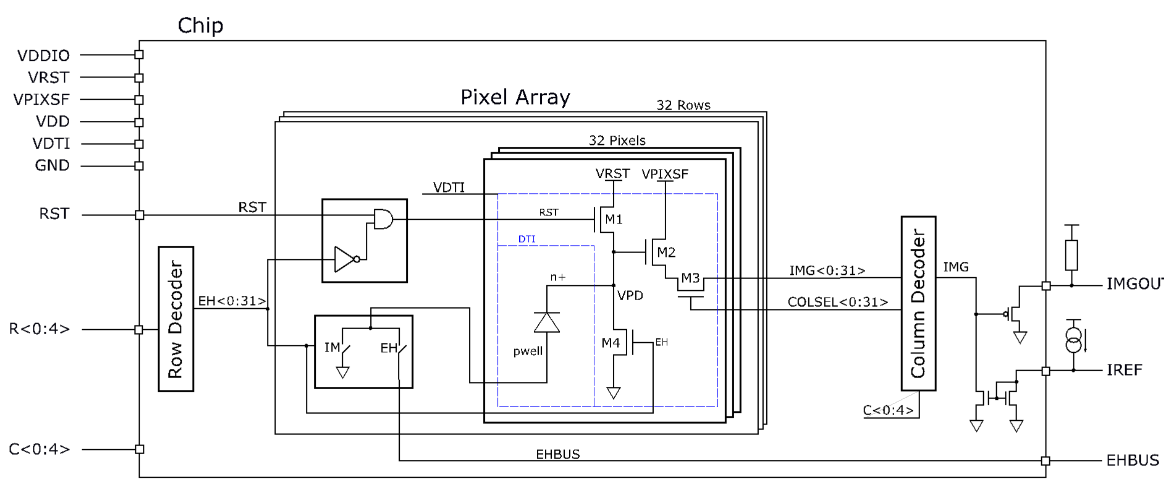

Figure 3: Chip block diagram. Control signals driven from FPGA and output measured using external ADC.

IV. Characterization Setup

Tests were carried out using the setup shown in Figure 4. A sensor placed at distance d away from an integrating sphere with output port of diameter D emulates the light cone from a lens with an f-number given by d/D. The true illumination at the sensor plane has been measured using a luxmeter, prior to it being replaced with the sensor at the same distance.

Figure 4: Darkroom characterization setup. Opaque slide used in shading experiment in Results section C.

V. Results

A. Peak Power

Figure 5 shows the peak generated power by the pixel array, from three different spectra vs. the sensor plane illuminance. The array appears to perform best under a spectrum with high infrared content (low luminous efficacy), and significantly worse under a white LED which only emits visible light (high luminous efficacy).

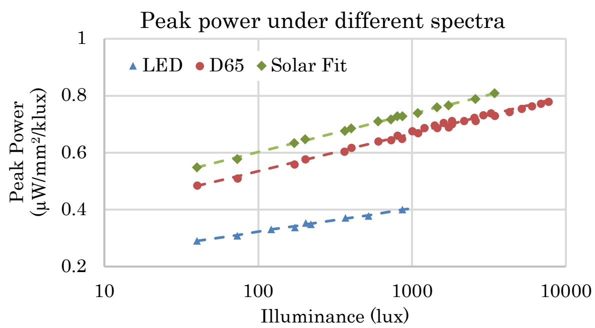

Figure 5: Plot of peak power generated vs. lux for three different spectra from Figure 1

Considering the power in the illuminating spectrum instead, the photovoltaic conversion efficiency is plotted in Figure 6. Efficiency under LED illumination is slightly higher than under broadband spectra.

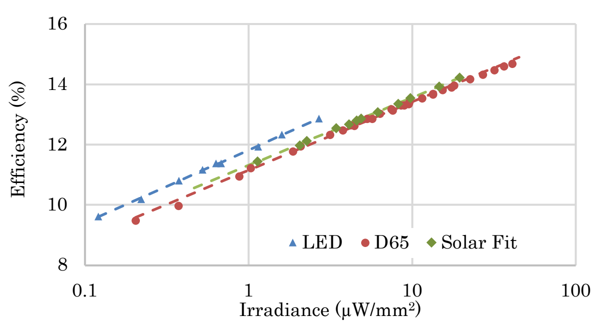

Figure 6: Photovoltaic conversion efficiencies for the spectra used.

The spectral responsivity of the photovoltaics has been measured using narrowband LEDs and is shown along with the ideal, 100% QE case in Figure 7.

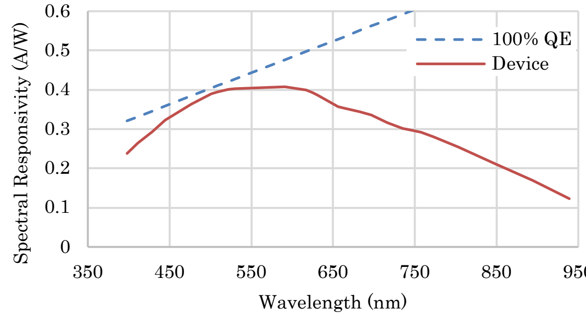

Figure 7: Spectral Responsivity

B. Image Capture and Energy Harvesting

The image projected on the array leaves some parts darker than others, affecting the overall power generation. Table 2 shows a few different scenes captured and the corresponding peak power generated during capture.

The illumination was kept constant between pairs of images *Logo* & *QR* and *Window* & *Person*, with the drop in power in each pair corresponding to the drop in the mean frame signal.

Logo	*QR*	*Window*	*Person*	*Hill*
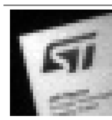	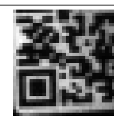	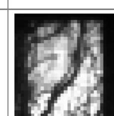	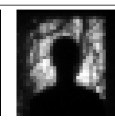	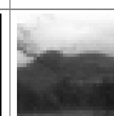
15.8nW	9.2nW	55nW	26nW	62nW
4000 lux on target		*330 lux		*5000 lux
f/3.4 lens, LED lamp.		f/2.8 lens, overcast daylight		

*Table 2: Captured images and corresponding power generation during capture. *light level measured at PCB using handheld luxmeter.*

C. Effect of Shading

To help quantify the effect that the specific target being imaged has on power generation, the sensor was partially shaded by an opaque slide, placed between the sensor and the integrating sphere port.

When all pixel diodes are connected in parallel, the peak power generation depends only on the average irradiance on the array, following the mean of the image signal closely, as shown in Figure 8.

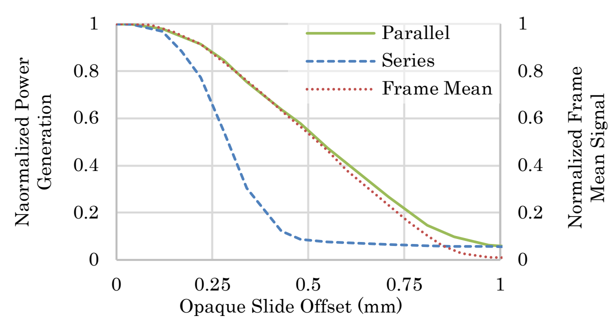

Figure 8: Peak generated power vs. increasingly shaded light field for parallel and series modes.

	Cevik [2]	Chiou [8]	Ay [1]	Park [4]	This work
Pixel type	4T EHI APS	PWM	4T EHI APS	3T hole based	4T EHI APS
Diode Type	IM: n+/psub EH: nwell/psub	IM: n+/pwell EH: d-nwell/pwell	IM: nwell/psub EH: p+/nwell	IM: p+/nwell EH: nwell/psub	BSI+DTI
Pixel Pitch	14μm	7.6μm	21μm	5μm	22.4μm
Array	96×96	256×192	54×50	100×90	32×32
Array area (mm^2)	1.806	2.84	1.19	0.225	0.514
Fill Factor	30%	30.8%	IM: 62% EH: 32%	IM: 46% EH: 94%	98%
EH/IM Operation	2 diodes per pixel	Frame-level, time multiplexed	Frame-level, time multiplexed	Junction depth	Row-level, time multiplexed
Power Generation (full array)	31.36μW (@60klux)	14μW (@60klux)	3.35μW (@60klux)	13.72μW (@60klux)	3.12μW (@7.7klux D65)
Power Generation (nW/klux/mm^2)	289 (@60klux)	82.2 (@60klux)	46.8 (@60klux)	998 (@60klux)	736* (@1klux solar) 667* (@1klux D65) 404* (@1klux LED)
Efficiency (%)	n/a	n/a	9.4%	n/a	9-15%

*Interpolated using a logarithmic fit from Figure 5.

Table 3: Comparison versus state-of-the-art EH pixels.

The same test has been repeated using a chip from [9] which has 4 equal area diodes connected in series. The peak power when uncovered is the same as for the parallel connection case, but drops to near minimum as soon as a single level of the photovoltaic stack is shaded and its current reduced. To maintain power generation in a series connected stack, the diode pattern must not match the image pattern being projected since this will have a disproportionally negative effect on the power generation.

VI. Discussion

The amount of power available when harvesting in the focal plane of a lens is very small and very fast lenses are needed to generate useful amounts of power. Modules with apertures around f/1.5 are now commercially available and are likely necessary to make this form of device possible. Using the hypothetical scene and lens from the initial example in Section II, but illuminated with 1000lux, a 1/3" format array (17.3mm^2) could generate between 270nW and 512nW, depending on the spectrum.

Some increase could be expected from increasing the p-epi thickness, improving the responsivity around red and infrared, however the benefit in indoor scenarios would limited since modern artificial light sources do not emit strongly in IR.

In Table 2, there is a large difference in illuminance between images *Window* and *Hill*, but little difference in generated power. This is due to different fields of view of the luxmeter and sensor. Evaluation could be improved by using a luminance meter instead.

VII. Conclusion

The theoretical bounds for energy harvesting have been evaluated, and depend primarily on the lens used. A new implementation of an EHI pixel has been studied, with focus on its power generation capabilities at realistic light levels. Power generation efficiency has been shown to be dependent on the illumination level and spectrum. The pixel array generated a peak power of 62nW when capturing a real, outdoor daylight scene. Deep trench isolation, as used in this testchip, is a promising process feature for future energy harvesting imagers, allowing for high voltage generation without charge pumps and new pixel implementations.

References

[1] S. U. Ay, "A CMOS energy harvesting and imaging (EHI) active pixel sensor (APS) imager for retinal prosthesis," *IEEE Trans. Biomed. Circuits Syst.*, vol. 5, no. 6, pp. 535–545, 2011.

[2] I. Cevik and S. U. Ay, "A 0.8V 140nW low-noise energy harvesting CMOS APS imager with fully digital readout," *Proc. IEEE 2014 Cust. Integr. Circuits Conf. CICC 2014*, pp. 5–8, 2014.

[3] I. Cevik and S. U. Ay, "An Ultra-Low Power Energy Harvesting and Imaging (EHI) Type CMOS APS Imager with Self-Power Capability," *IEEE Trans. Circuits Syst. I Regul. Pap.*, vol. 62, no. 9, pp. 2177–2186, 2015.

[4] S. Y. Park, K. Lee, H. Song, and E. Yoon, "Simultaneous Imaging and Energy Harvesting in CMOS Image Sensor Pixels," *IEEE Electron Device Lett.*, vol. 39, no. 4, pp. 532–535, 2018.

[5] J. H. Ko, M. F. Amir, K. Z. Ahmed, T. Na, and S. Mukhopadhyay, "A Single-Chip Image Sensor Node with Energy Harvesting from a CMOS Pixel Array," *IEEE Trans. Circuits Syst. I Regul. Pap.*, vol. 64, no. 9, pp. 2295–2307, 2017.

[6] W. D. Leon-Salas, T. Fischer, X. Fan, G. Moayeri, and S. Luo, "A 64×64 image energy harvesting configurable image sensor," *Proc. - IEEE Int. Symp. Circuits Syst.*, vol. 2016–July, pp. 1914–1917, 2016.

[7] N. Couniot, G. De Streel, F. Botman, A. K. Lusala, D. Flandre, and D. Bol, "A 65 nm 0.5 V DPS CMOS Image Sensor With for Ultra-Low-Power SoCs," *IEEE J. Solid-State Circuits*, vol. 50, no. 10, pp. 2419–2430, 2015.

[8] A. Y. C. Chiou and C. C. Hsieh, "A 137 dB Dynamic Range and 0.32 V Self-Powered CMOS Imager With Energy Harvesting Pixels," *IEEE J. Solid-State Circuits*, vol. 51, no. 11, pp. 2769–2776, 2016.

[9] F. Kaklin, J. M. Raynor, and R. K. Henderson, "High Voltage Generation Using Deep Trench Isolated Photodiodes in a Back Side Illuminated Process," *2018 IEEE Int. Electron Devices Meet.*, pp. 743–746, 2018.